Excerpt from the Proceedings of the 2011 COMSOL Conference in Boston

Coupled Magnetodynamic and Electric Circuit Models for Superconducting Fault Current Limiter

Lukas Graber[*,1], Jozef Kvitkovic[1], Tim Chiocchio[1], Michael Steurer[1], Sastry Pamidi[1] and Alexander Usoskin[2]
[1]Center for Advanced Power Systems, Florida State University
[2]Bruker Energy & Supercon Technologies, Inc.
*Corresponding author: Center for Advanced Power Systems, 2000 Levy Avenue, Tallahassee, FL 32310, USA, graber@caps.fsu.edu

Abstract: Finite element models, which include the shielding characteristics of superconductors are often complex and would currently not allow to study three dimensional models of devices of complex geometry such as fault current limiters. The authors propose instead a model based on variable electric conductivity, which is suitable to simulate magnetic field characteristics of inductive superconducting fault current limiters. It also enables such simulations to be combined with an electric circuit model. A benchtop demonstration module of an inductive superconducting fault current limiter has been dimensioned and optimized by a coupled magnetodynamic and electric circuit model. Based on this model, this fault current limiter was built for model validation and refinement as well as for additional laboratory experiments. The results from the simulation model exhibited good agreement with the measurements in the laboratory.

Keywords: Magnetodynamic model, electrical circuit, superconductivity, fault current limiter

1. Introduction

A superconducting fault current limiter (SFCL) is a device to be used in electric power systems to limit the magnitude of fault currents in the event of a short circuit. SFCLs are expected to be particularly useful in power grids with ever increasing levels of fault currents, primarily due to increases in power generation capacity and, particularly at the distribution level, the observed increase in penetration of local generation provided via rotating machinery. Currently, various designs of SFCLs are under development. Among the different types of SFCL, the inductive SFCL (iSFCL) is especially interesting since it is expected to have significant operational advantages stemming from its design features [1]. The iSFCL does not need current leads and hence does not have the heat leak from the ambient and Joule's heating from the current leads. This significantly lowers consumption of the liquid nitrogen (LN2) compared to other types of SFCLs.

Figure 1 depicts the basic conceptual design of an iron core less iSFCL. The primary coil is connected electrically in series with the load impedance Z_{Load}. In normal operation, the superconducting (SC) rings shield part of the volume inside the primary coil by carrying a counter-acting current, thereby reducing its inductance. In a fault condition, the increasing current in the primary coil causes a corresponding increase in the magnetic field at the SC rings. By design, the superconductor can only shield the field up to a certain value at which it quenches to the normal state. This transition significantly increases the inductance of the primary coil and thus limits the current in the external circuit (i.e. the power grid).

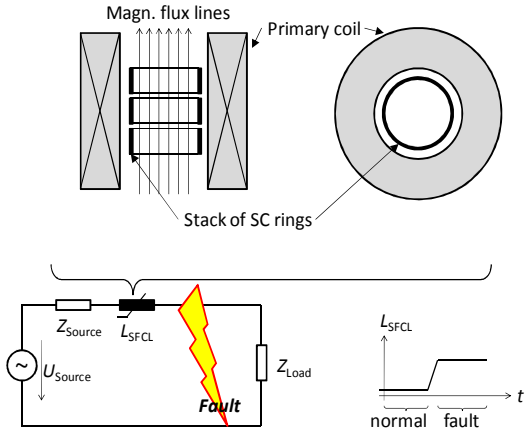

Figure 1. Schematic drawing of the inductive superconducting fault current limiter without iron core (top) along with the electric circuit in which it is embedded (lower left) and a graph showing the idealized change of the primary inductance (lower right).

The shielding properties of single rings of second generation high temperature superconducting (HTS) tape have been measured. This is the same type of ring used for the single-phase benchtop demonstration module of an iSFCL described in this paper. The magnetic shielding factor S is defined as a function of the applied external flux density B_{ext} (measured without ring) and the internal flux density B_{int} (measured inside the ring when it is in place):

$$S = \frac{B_{\text{ext}} - B_{\text{int}}}{B_{\text{ext}}} \cdot 100\% \quad (1)$$

The shielding factor is a function of the magnitude of the external magnetic field. The ring was immersed in LN2 at a temperature of 77 K. The frequency of the sinusoidal external magnetic field was 57 Hz. The result in Figure 2 shows a shielding factor for approximately 78% for a flux density below 8.26 mT. The shielding properties are almost completely lost above this value where the factor drops to approximately 6%. This abrupt change resulted in the idea to model the magnetic field inside an iSFCL by a finite element analysis (FEA), where the ring abruptly changes its characteristics depending upon the external magnetic flux density. This can be achieved simply by changing the electrical conductivity of the ring. The induced voltage on the ring results in a conductivity-dependent current. The interaction of the magnetic field by the ring with the magnetic field by the primary coil results in partial shielding. This approach works without the use of the power law, which is so often cited in applied superconductivity research [2].

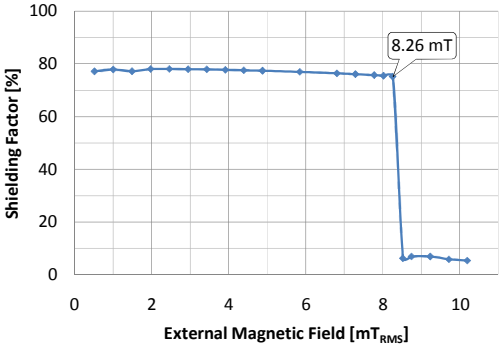

Figure 2. Magnetic shielding factor of the superconducting ring as a function of applied field magnitude.

2. Finite Element Model

The authors consider FEA as a powerful tool to dimension, design, and optimize the magnetic field behavior of iSFCL. The FEA model was coupled with a SPICE circuit simulation, which drives the current in the primary coil of the iSFCL. The coupling of FEA with the circuit is bidirectional. The model was implemented in COMSOL Multiphysics 4.1. The study was conducted over three time periods: From −17 ms to 68 ms, from 68 ms to 230 ms, and from 326 ms to 700 ms, each with a resolution of 1 ms.

2.1 Governing Equations

The governing equations of the finite element model were magnetic field equations (Ampère's Law) in time-dependent form:

$$\sigma \frac{\partial \mathbf{A}}{\partial t} + \nabla \times \mathbf{H} - \sigma\, \mathbf{v} \times \mathbf{B} = \mathbf{J}_{\text{e}}$$
$$\mathbf{B} = \nabla \times \mathbf{A} \quad (2)$$

with electric conductivity σ, magnetic vector potential $\mathbf{A}$, magnetic field $\mathbf{H}$, magnetic flux density $\mathbf{B} = \mu_0 \mathbf{H}$, velocity vector $\mathbf{v}$, and external current density $\mathbf{J}_{\text{e}}$. The model did not incorporate any moving objects resulting in a zero velocity vector $\mathbf{v} = 0$.

2.2 Geometry and mesh

The geometry was 2D axisymmetric. It consisted of three domains: A thin superconducting layer on a ring, a multi-turn coil domain, and the surrounding space (Figure 3).

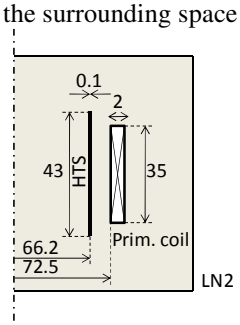

Figure 3. Geometry of the FEA model (dimensions in [mm]; not drawn to scale).

The superconducting layer was only 1 µm thick. In order to reduce the number of mesh elements required for such a thin structure, the

thickness was artificially increased to 100 µm. The conductivity of the material was decreased by a factor of 100 to compensate for the increased cross section. The ring had an inner diameter of 132 mm and a height of 43 mm.

The multi-turn coil domain contained the primary winding. It consisted of 60 turns of copper wire, tightly wound in a coil of an inner diameter of 145 mm, a thickness of 2 mm, and a height of 35 mm.

The surrounding space was a cylinder of 1 m height and 1 m diameter. It accommodated the ring and the coil in its center.

The mesh was not critical in terms of quality and resolution. Therefore it was automatically generated (in COMSOL terms: "physics-controlled mesh") with medium element size ("Normal"). This resulted in 10,189 triangular mesh elements. The minimum element quality was 0.7145.

2.3 Initial and boundary conditions

The initial values for the magnetic vector potential were zero. The surrounding LN2 domain showed magnetic insulation ($\mathbf{n} \times \mathbf{A} = 0$) on its boundary.

The multi-turn coil was coupled with an electrical circuit modeled by COMSOL's internal SPICE solver. This circuit consisted of three blocks: An equivalent representation of a three-phase frequency converter (Figure 4 left), an equivalent circuit of the single-phase step down transformer (Figure 4 center), and the impedance of the multi-turn coil domain along with a parallel resistor for protection purposes (Figure 4 right). The multi-turn coil domain was part of the FEA model of the iSFCL.

The step down transformer was part of the laboratory setup. The values of the components in its equivalent circuit were determined by open circuit and short circuit tests in the laboratory. The model was validated by comparison of laboratory measurements with a simulation of the equivalent circuit using the software package PSCAD/EMTDC 4.2.1. In order to refer all component values to the secondary side, the values were adjusted according to the transformer ratio of 7.5:1.

The 25 kW power electronics inverter with its filter and grounding components was also part of the laboratory setup. The component values in the equivalent circuit corresponded (in slightly simplified form) to the actual implementation in hardware. Again all values were adjusted according to the transformer ratio.

The electric circuit consisted of 13 nodes including the ground node. All components had constant values except for the impedance of the SFCL, which was calculated in the finite element model, and the source voltages. The three phase voltage source was in Y circuit configuration. The base voltage of the sinusoidal 60 Hz sources was 12 V_{RMS} (phase to phase). The pulse voltage, simulating the short circuit of the power system, had a length of ten cycles (167 ms) and a magnitude of 84 V_{RMS}. The voltage of the inverter was adjustable from 0 V_{RMS} to 240 V_{RMS}.

2.4 Materials

The electric conductivity of the HTS ring was adjusted externally. In superconducting state, it was assumed to be approximately $2.5 \cdot 10^{14}$ S/m. However, in order to compensate

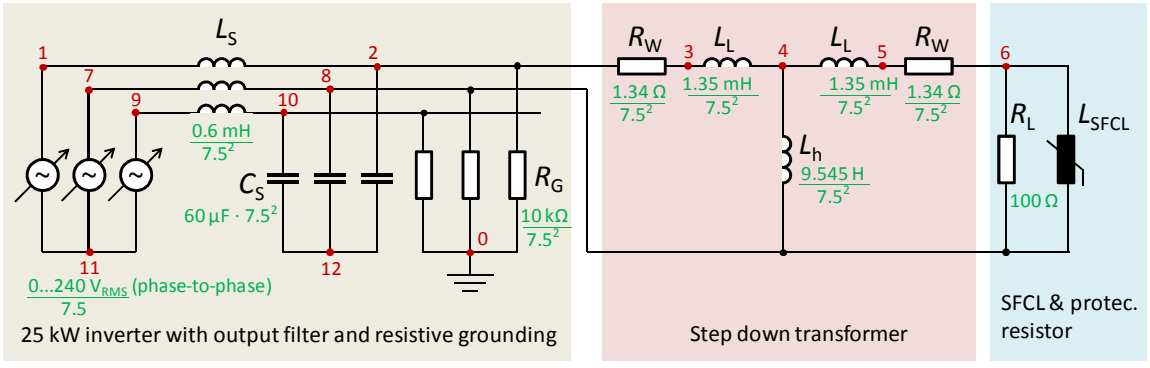

Figure 4. Equivalent circuit diagram of the test of the single phase SFCL; numbers in red indicate the node numbers for the SPICE model.

for the 100 times increase of cross section, the conductivity was reduced to $2.5 \cdot 10^{12}$ S/m. In quenched state, the conductivity was set to $2.5 \cdot 10^{-2}$ S/m, which can be interpreted as an almost ideal insulator. The quench process was observed to be almost instantaneous and occured immediately at the moment the voltage pulse (simulated fault) was applied. The conductivity was therefore changed from $2.5 \cdot 10^{12}$ S/m to $2.5 \cdot 10^{-2}$ S/m without any delay or transition time. The recovery process was also fast, however delayed by typically several power frequency cycles. Experiments with the iSFCL showed that the recovery time is a function of pulse length and amplitude. For a pulse of ten cycles length and 84 V_{RMS}, the recovery occurred eleven cycles after the pulse stopped. Relative permeability μ_r and the relative permittivity ε_r were both unity. Figure 5 provides an overview with the timeline of the time dependent parameters.

The conductor in the multi-turn coil domain was implemented as a copper wire of 0.82 mm^2 cross section (1.02 mm diameter). The conductivity was $5.0 \cdot 10^8$ S/m at a temperature of 77 K. Relative permeability μ_r and relative permittivity ε_r were again both unity.

The surrounding medium was liquid nitrogen at 77 K and ambient pressure: $\mu_r = 1$; $\varepsilon_r = 1.4$; $\sigma = 0$ S/m.

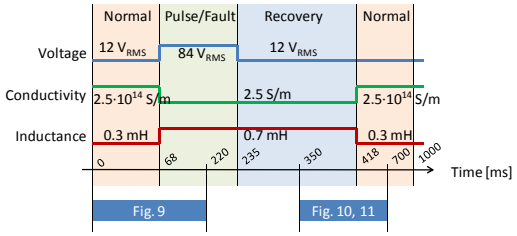

Figure 5. Applied voltage, HTS conductivity and inductance of the iSFCL as a function of time.

2.5 Solver Settings

Even though the electric conductivity of the ring changed by 14 orders of magnitude, no difficulties regarding convergence were observed. The solver settings remained untouched on default values. The amplitude of the voltage sources was kept constant during a simulation run, reducing the risk of convergence difficulties.

2.6 Simulation Results

Figure 6 shows the magnetic flux density at $t = 400$ ms, which was after the voltage pulse but before the HTS recovered and was therefore in quench state. The current in the primary coil was at its maximum value. The ring did not carry significant current, which resulted in no interaction with the external magnetic field. In other words, the ring was transparent for the magnetic field.

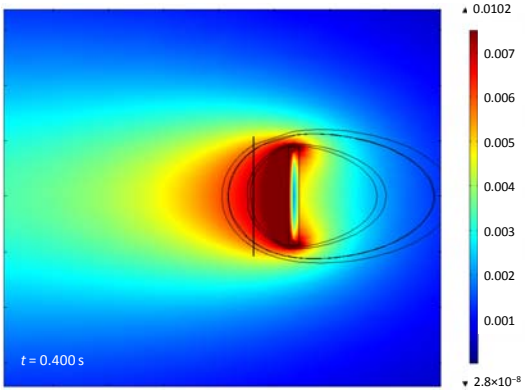

Figure 6. Simulated magnetic flux density in the experimental setup during quench of the HTS ring ($t = 400$ ms).

In contrast to the above case, Figure 7 shows the magnetic flux density at $t = 432$ ms when the HTS recovered. It was again during maximum current. The HTS ring was superconducting and carried significant current density, canceling the magnetic field. This effectively shielded the inner space from magnetic field.

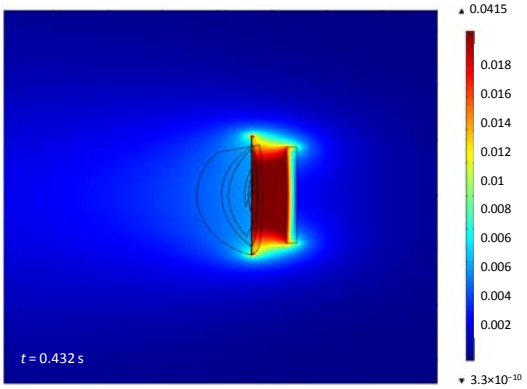

Figure 7. Simulated magnetic flux density in the experimental setup after the HTS ring recovered ($t = 432$ ms).

3. Experimental Validation of the Model

3.1 Laboratory Setup of the Experiment

This benchtop demonstration module was based on a single HTS ring. The ring has an inner diameter of 132 mm and a height of 43 mm. The 1 µm thick HTS layer was made of a second generation superconductor on an electrically non-conducting material. The assembly did not incorporate a shunt ring. The primary coil was made from enameled copper wire on a G10 tube, a non-conducting composite material of woven fiberglass cloth with an epoxy resin binder. The HTS ring was located inside the primary coil. The whole assembly was in an open LN2 bath in a Styrofoam container. Even though this would not be suitable for a power systems application, it was convenient for these laboratory tests. Figure 8 shows the benchtop demonstration module with the HTS ring lifted above the container. For this photograph, the container was not filled with LN2.

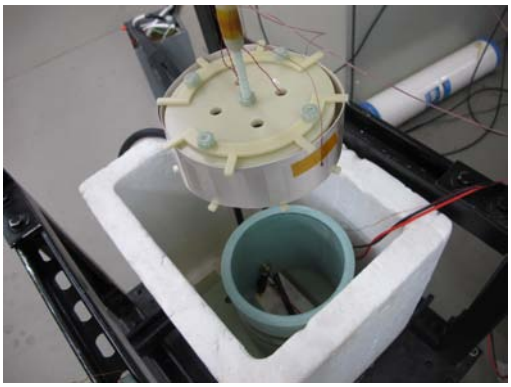

Figure 8. Styrofoam container with the primary coil on a G10 former and the HTS ring lifted up.

The primary coil of the iSFCL was connected to the secondary of a step down transformer with a 7.5:1 turns ratio. The primary of the transformer was connected between two phases of a three-phase 25 kW inverter. A 100 Ω power resistor was connected in parallel to the transformer output to add a certain resistive load to the inverter. It also acted as a protection element for the inverter in case the coil would fail.
The inverter was controlled to supply a certain sinusoidal voltage just below the level at which the HTS ring would quench. For this setup this steady-state voltage was 12 V_{RMS} (phase-to-phase voltage between the two phases of the inverter). To test the current limiting capabilities of the iSFCL, the amplitude was increased for a short amount of time. A typical pulse length was ten power frequency cycles (167 ms at 60 Hz) for a voltage of 84 V_{RMS}. Such a pulse always started at a zero voltage crossing because of two reasons: It facilitated reproducibility of the tests and it typically corresponds to the case with maximum fault current in power systems with large X/R [3]. The rate of change of voltage amplitude was limited to 72 kV/s. After the pulse, the voltage was reduced again to its initial value.

3.2 Results of the Experiment and Comparison with Simulation Results

Figure 9 shows voltage and current in the primary coil shortly before and during the pulse. The current shows a certain asymmetry (DC offset) during the first two cycles of the pulse. The moment of quench of the HTS ring occurs within the first quarter-cycle of the voltage pulse. The simulation (blue curve) and measurement (red) plots show good agreement. It should be noted that the simulation run was performed in two phases and then the two data sets were joined together since the model solution did not converge with simultaneously changing voltage magnitude and HTS ring conductivity.

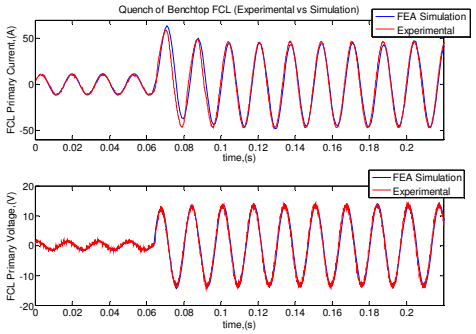

Figure 9. Simulated (blue) and measured (red) current (top) and voltage bottom) in the primary coil of the iSFCL benchtop demonstration module during the onset of the pulse.

The transition from quenched to normal state of the HTS ring is depicted in Figure 10. Again, current and voltage in the primary coil show a remarkably similar shape in simulation (blue) and measurement (red).

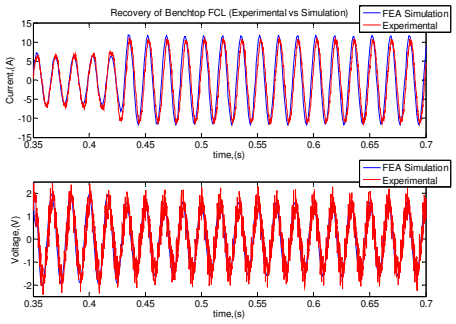

Figure 10. Simulated (blue) and measured (red) current (top) and voltage (bottom) in the primary coil of the iSFCL benchtop demonstration module during the recovery from quenched to superconducting state of the HTS ring.

For power engineering aspect, one of the most important parameters of an iSFCL is its change of inductance. The inductance can be obtained as a function of current $i_{FCL,RMS}$ and voltage $u_{FCL,RMS}$ across the device:

$$L(t) = \frac{1}{2\pi f} \frac{u_{FCL,RMS}}{i_{FCL,RMS}} \sin(\theta_{i-v}) \qquad (3)$$

with θ_{i-v} the phase angle. The inductance of the iSFCL for both the experiment and simulation changes from approximately 0.7 mH in quenched state to 0.3 mH in superconducting state (Figure 11).

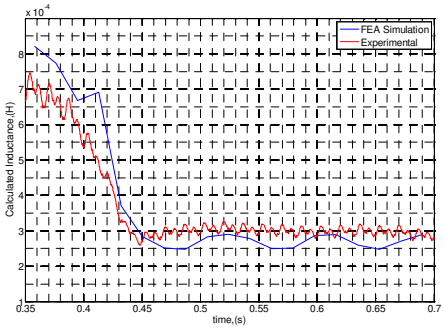

Figure 11. Calculated inductance during the transition from quenched to superconducting state for both simulation (blue) and measurement (red).

For the experimental data, the phase angle and RMS voltage and current are calculated using native functions in Real Time Digital Simulator (RTDS), used to control the power electronics inverter. For the simulation data, the phase angle and RMS are calculated by zero crossing detection and sliding window-based RMS, respectively. In both simulation and measurement the calculated values for inductance show some uncertainty. The simulation also has what appear to be a few outliers in the left side of the plot but the results in general show good agreement.

4. Conclusion

The proposed approach to model the shielding properties of superconductors in fault current limiters by changing the electric conductivity showed promising results. It resulted in efficient simulation models, which allowed three dimensional geometries and coupling with electrical circuits. The simulation results showed a good agreement with measurements conducted at a benchtop demonstration module of a fault current limiter. The authors conclude that such an approach is feasible and appropriate for designing and dimensioning iSFCLs regarding its magnetic and power system aspects.

For future tests, the inverter will allow the iSFCLs to be embedded in a simulated power system using the power hardware-in-the-loop (PHIL) concept. A real time computer simulator reads the voltage across the primary coil and imposes the current from the simulated power grid onto the iSFCL, thereby facilitating the dynamic interaction between the iSFCL and the simulated power grid by means of a power amplifier [4].

5. References

1. M. Chen et al., Fabrication and Characterisation of Superconducting Rings for Fault Current Limiter Application, *Physica C*, **282 – 287**, pages: 2639 – 2640 (1997)

2. H. Ueda et al., Thermal and magnetic characteristics of bulk superconductor and performance analysis of magnetic shielding type of superconducting fault current limiter, *IEEE Trans. on Applied Superconductivity*, Volume **11**, Issue 1, pages 2402 – 2405 (2001)

3. H. Saadat, Power System Analysis, 2nd Edition, *McGraw-Hill Companies, Inc*, **314 – 341** (2002)

4. C. Schacherer et al., Power Hardware-in-the-Loop Testing of a YBCO Coated Conductor Fault Current Limiting Module, *IEEE Trans. on Applied Superconductivity*, Volume **19**, Issue 3, Part 2, pages: 1801 – 1805 (2009)